APPENDIX 1

Gravity Data

Gravity anomalies reflect lateral variations of density, with gravity highs occurring over regions of relatively high densities, such as mountains composed of crystalline basement, and gravity lows occurring over large volumes of low-density materials, such as unconsolidated sediments. Large density contrasts between low-density rift-filling sediments, such as the Santa Fe Group, and older rocks make gravity data useful for defining the configuration of basins within the Rio Grande rift (Cordell, 1978; Daggett et al., 1986; Grauch et al., 2006).

Regional quality (1-5 km station spacing) gravity data were extracted from the PACES gravity database that is maintained by the University of Texas at El Paso (http://gis.utep.edu/) and supplemented with additional data acquired along two east-west transects. The PACES database consists of data collected over decades by many previous workers and was compiled as the result of a major cooperative effort between federal agencies and universities (Keller et al., 2006). Standard techniques (e.g., Blakely, 1995) reduce observed gravity data to complete Bouguer anomalies, including corrections for predicted gravitational attraction at the elevation and latitude of the observation point (theoretical and free air corrections), effects of homogeneous masses underneath each point (Bouguer correction), and effects of topographic masses (terrain corrections). The standard reduction density of 2670 kg/m^3 (Hinze, 2003) was used for the Bouguer and terrain corrections. A regional field based on the isostatic effect of regional topography was additionally removed to better represent upper-crustal density variations (Simpson et al., 1986; Blakely, 1995). Computation of isostatic residual anomalies requires estimates of crustal thickness and Moho density contrast, but these values do not need to be highly accurate to yield useful results. A Moho density contrast of 400 kg/m^3 and a normal (assuming ground surface at sea level) crustal thickness of 25 km constrain the calculation of isostatic residual anomalies.

Aeromagnetic Data

Data from two high-resolution total-field aeromagnetic surveys (200 meter flight line spacing, 100 meters above the ground) acquired during 2004 and 2005 were draped to a surface 100 meters above the ground and merged to create an aeromagnetic map of the study area (Bankey et al., 2005, 2006). A reduction-to-pole transformation, which is a standard geophysical technique to model center anomalies over their sources, was applied to the aeromagnetic data using an inclination of 64 degrees and declination of 10 degrees (Baranov and Naudy, 1964; Blakely, 1995).

Aeromagnetic data were used to identify potential buried faults with limited or no surface expression in Sunshine Valley. Magnetic contrasts that correspond to geologic contacts and faults produce linear and often subtle aeromagnetic anomalies, due to juxtaposition of units with different magnetic properties. The patterns of these contrasts can be enhanced in map view using transformations of the reduced-to-pole aeromagnetic anomalies, especially the horizontal gradient magnitude (HGM) and first vertical derivative (Grauch and Hudson, 2007). These methods were applied to the reduced-to-pole aeromagnetic data to identify patterns of magnetic contrasts that are possibly related to faulting. An analysis conducted independently from the mapping of fault scarps on the surface (Plate 1). The Sunshine Valley fault zone has a well expressed aeromagnetic signature that is in close proximity to mapped fault scarps.

Rock Property Information

Laboratory measurements of rock densities and magnetic susceptibilities from eleven sites were performed to constrain the geophysical model (presented below). Rocks that crop out in the Sangre de Cristo Mountains have an estimated average density of 2680 kg/m^3, however basement rock densities under the western part of the study region are unknown because they are not exposed. Volcanic rocks of the TPVF may have remanent magnetizations of 1-10 A/m (Grauch and Keller, 2004), although magnitudes of 1 A/m are typical for the Servilleta Basalt in the Rio Grande gorge (Brown et al., 1993), and values as high as 8 A/m are reported for San Pedro Mesa, north of our study area (M. Hudson, personal comm., 2007). Magnetic susceptibilities measured on Servilleta Basalt samples range from 2-14 x 10^{-3} SI units with an average of 7 x 10^{-3} SI units. The basalt has a strongly vesicular texture, resulting in lower measured densities (~2640 kg/m^3) than normally observed for massive basalts. The estimated density of the Santa Fe Group basin fill is based on well logs in the Albuquerque and Española Basins to the south and assumed to be valid for the northern Rio Grande rift (Grauch et al., 2006).

References

Cordell, L., 1978, Regional geophysical setting of the Rio Grande rift: Geological Society of America Bulletin, v. 89, p. 1073-1090.

Bankey, V., Grauch, V.J.S., Webbers, A., and PRJ, Inc., 2005, Digital data and derivative products from a high-resolution aeromagnetic survey of the central San Luis basin, covering parts of Alamosa, Conejos, Costilla, and Rio Grande Counties, Colorado, and Taos County, New Mexico: U.S. Geological Survey Open-File Report 2005-1200, available at http://pubs.usgs.gov/of/2005/1200/.

Bankey, V., Grauch, V. J. S., Drenth, B., and Geophex, Inc., 2006, Digital data from the Santa Fe East and Questa-San Luis helicopter magnetic surveys in Santa Fe and Taos Counties, New Mexico, and Costilla County, Colorado: U.S. Geological Survey Open-File Report 2006-1170, available at http://pubs.usgs.gov/of/2006/1170/.

Baranov, V., and Naudy, H., 1964, Numerical calculation of the formula of reduction to the magnetic pole: Geophysics, v. 29, p. 67-79.

Blakely, R.J., 1995, Potential Theory in Gravity and Magnetic Applications, Cambridge University Press, 441 p.

Daggett, P.H., Keller, G.R., Morgan, P., and Wen, C.L., 1986, Structure of the southern Rio Grande rift from gravity interpretation: Journal of Geophysical Research, v. 91, p. 6157-6167.

Grauch, V.J.S., and Keller, G.R., 2004, Gravity and aeromagnetic expression of tectonic and volcanic elements of the southern San Luis Basin, New Mexico and Colorado, *in* Brister, B.S., Bauer, P.W., Read, A.S., and Lueth, V.W., eds., Geology of the Taos Region: New Mexico Geological Society, 55th Annual Field Conference, Guidebook, p. 230-243.

Grauch, V.J.S., Sawyer, D.A., Minor, S.A., Hudson, M.R., and Thompson, R.A., 2006, Gravity and aeromagnetic studies of the Santo Domingo basin area, New Mexico, *in* Minor, S.A., ed., The Cerrillos Uplift, the La Bajada Constriction, and Hydrogeologic Framework of the Santo Domingo Basin, Rio Grande Rift, New Mexico, U.S. Geological Survey Professional Paper 1720, p. 62-86.

Grauch, V.J.S., and Hudson, M.R., 2007, Guides to understanding the aeromagnetic expression of faults in sedimentary basins: Lessons learned from the central Rio Grande rift, New Mexico: Geosphere, v. 3, no. 6, p. 596-623.

Hinze, W.J., 2003, Bouguer reduction density: why 2.67?: Geophysics, v. 68, p. 1559-1560.

Keller, G.R., Hildenbrand, T.G., Hinze, W.J., and Li, X., 2006, The quest for the perfect gravity anomaly: Part 2 — Mass effects and anomaly inversion: Society of Exploration Geophysicists Technical Program Expanded Abstracts, v. 25, p. 864.

Simpson, R.W., Jachens, R.W., Blakely, R.J., and Saltus, R.W., 1986, A new isostatic residual gravity map of the conterminous United States with a discussion on the significance of isostatic residual anomalies: Journal of Geophysical Research, v. 91, p. 8348-8372.

APPENDIX 2
FAULT SCARP PROFILES
(see Plate 1 for locations)

Note: SH - Scarp height, the measurement from the crest of the scarp horizontally out and vertically down to the toe of the scarp.
SO - Surface Offset, the distance between the far-field slope of both the footwall and hanging wall sub-parallel surfaces.
Max Angle - the maximum slope of the fault scarp.

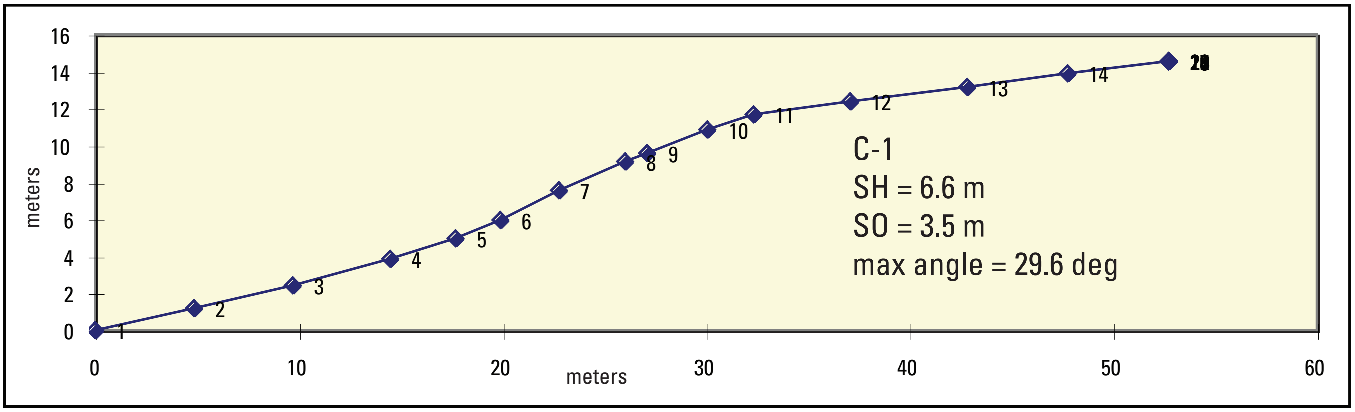

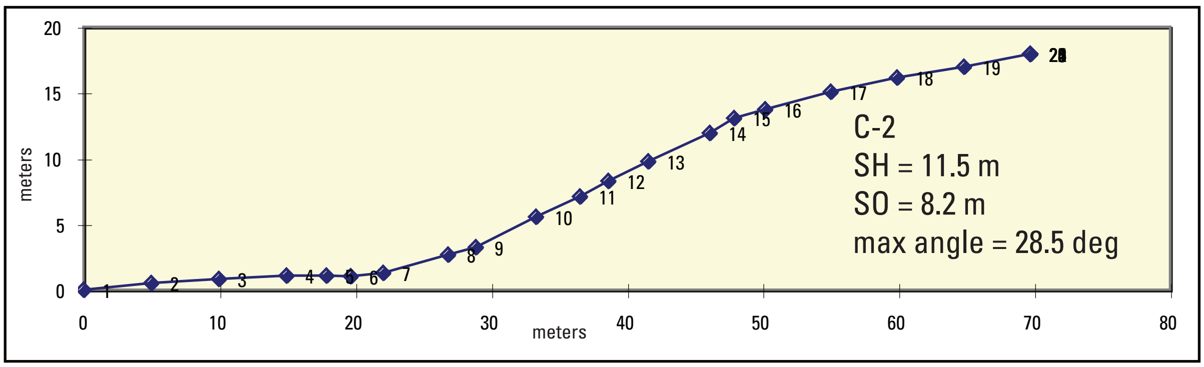

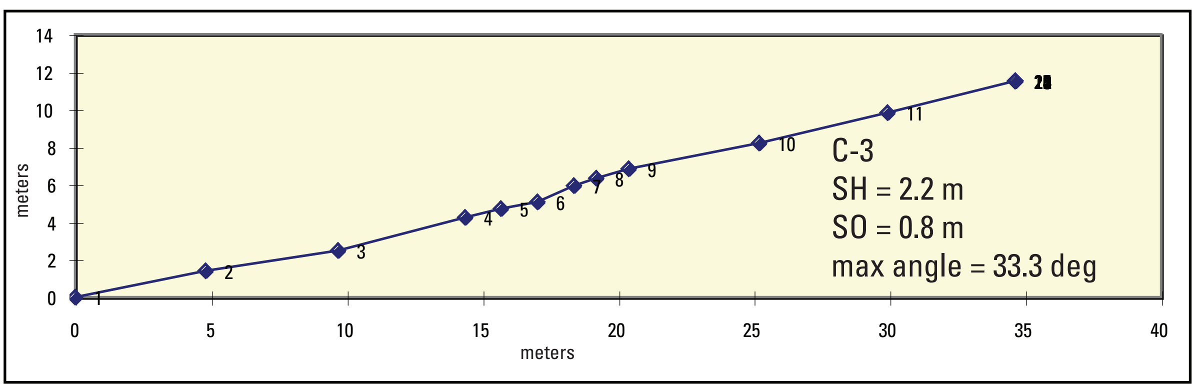

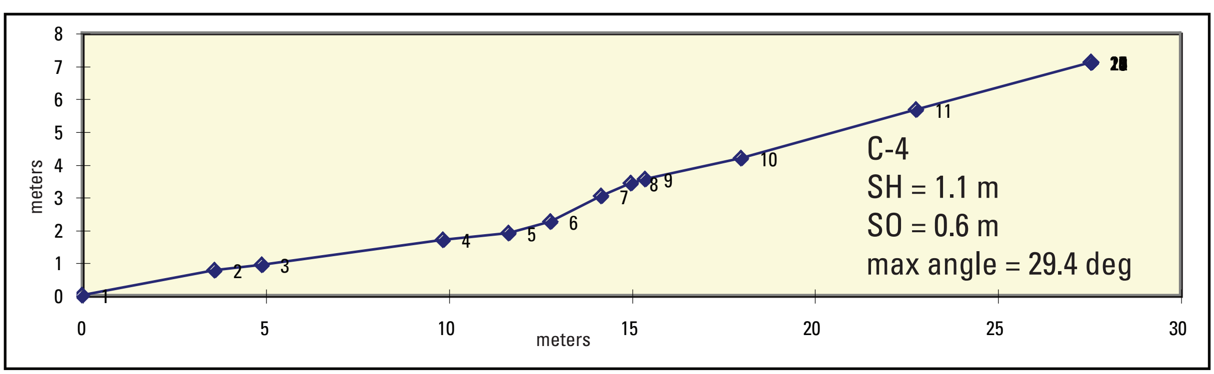

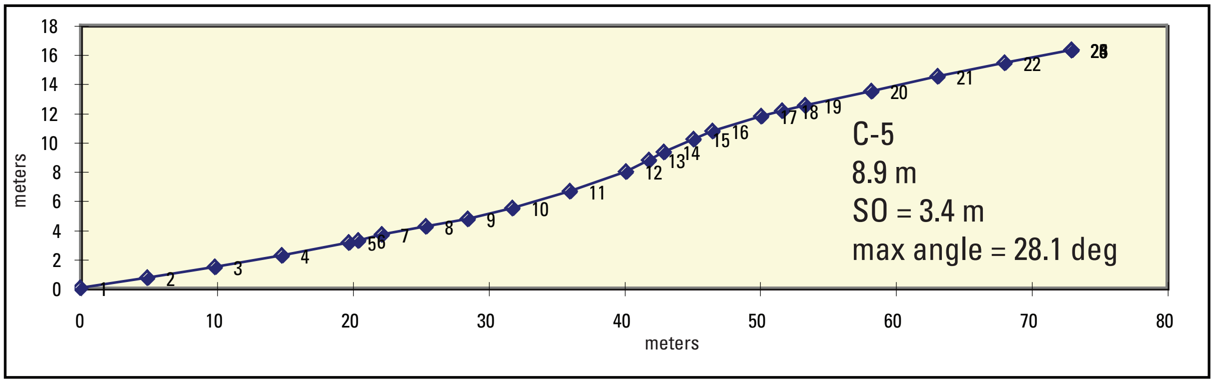
C-5
8.9 m
SO = 3.4 m
max angle = 28.1 deg
meters
meters

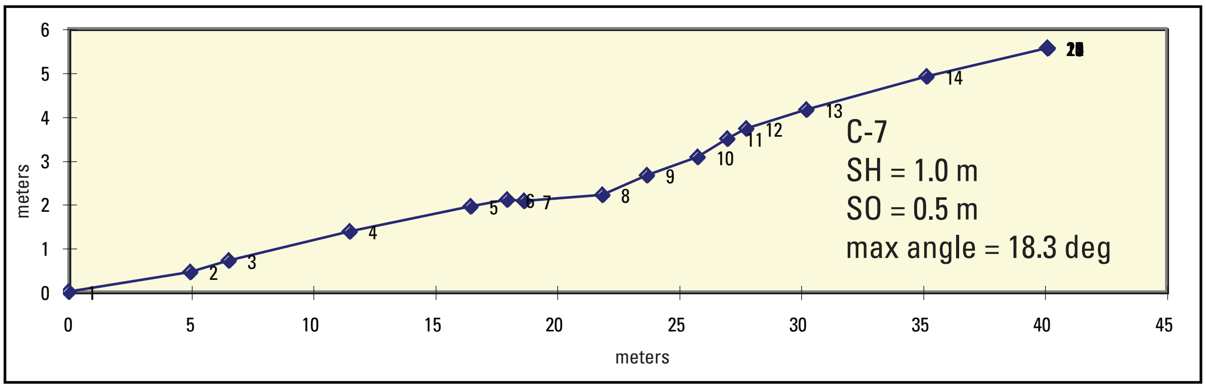
C-7
SH = 1.0 m
SO = 0.5 m
max angle = 18.3 deg
meters
meters

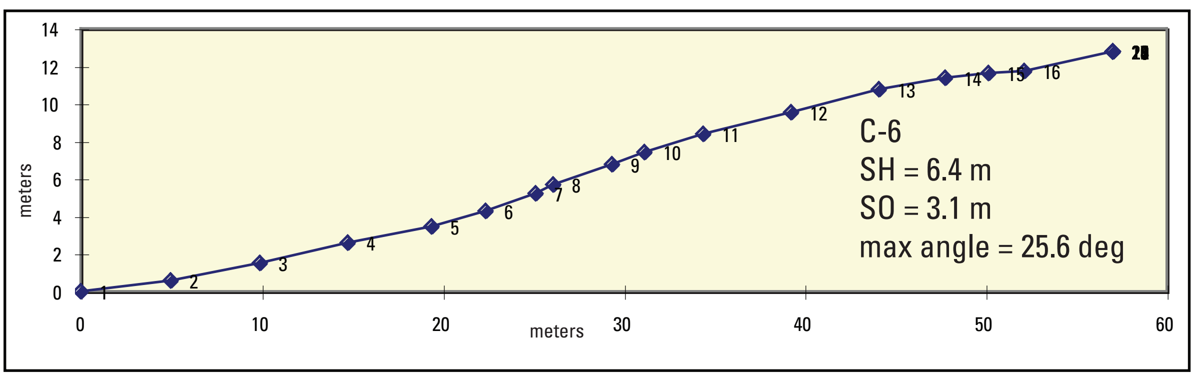
C-6
SH = 6.4 m
SO = 3.1 m
max angle = 25.6 deg
meters
meters

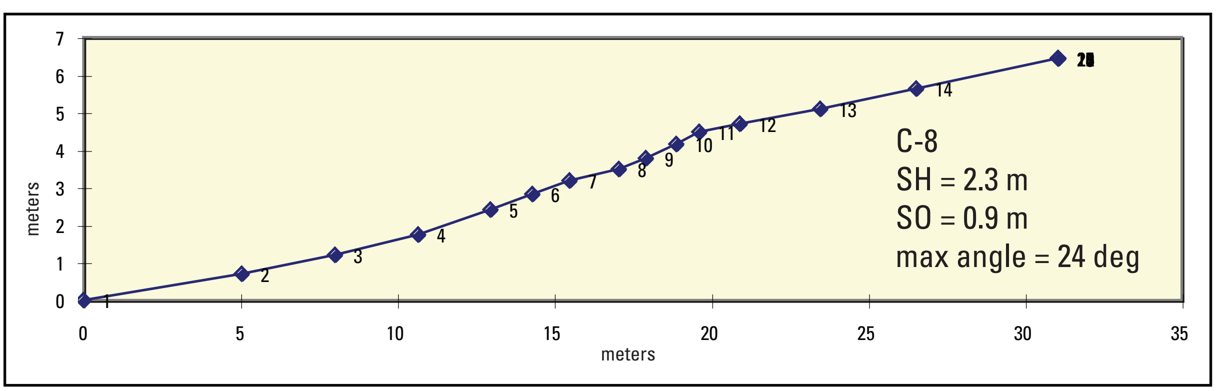
C-8
SH = 2.3 m
SO = 0.9 m
max angle = 24 deg
meters
meters

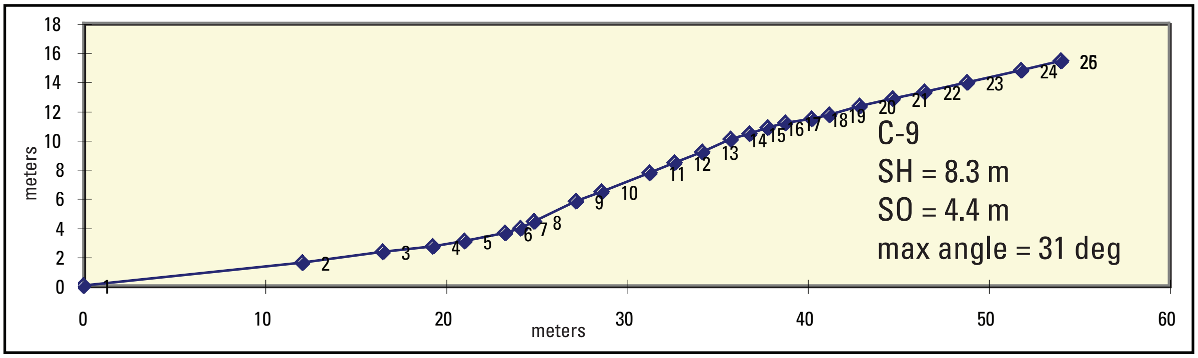
C-9
SH = 8.3 m
SO = 4.4 m
max angle = 31 deg
meters
meters

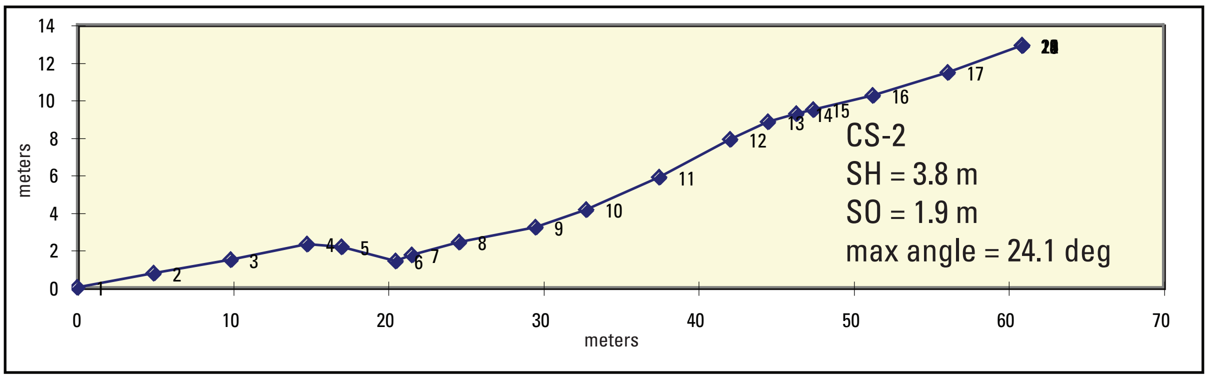
CS-2
SH = 3.8 m
SO = 1.9 m
max angle = 24.1 deg
meters
meters

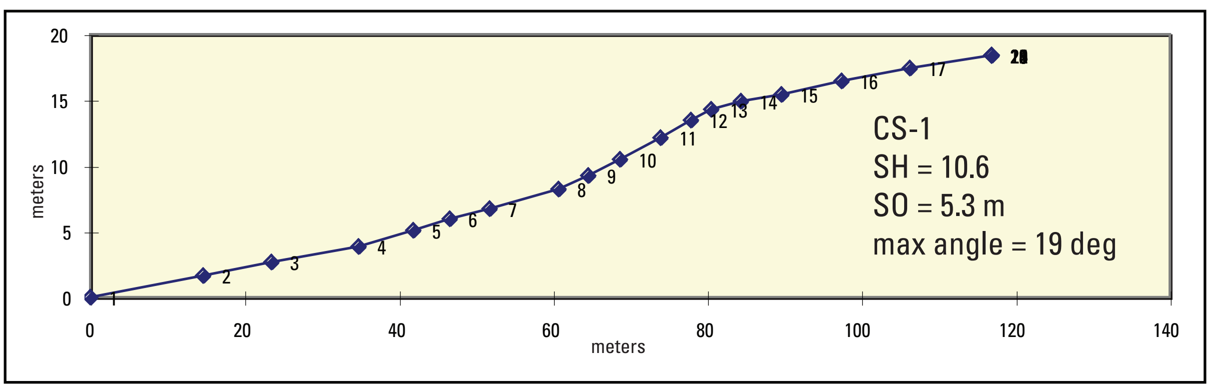
CS-1
SH = 10.6
SO = 5.3 m
max angle = 19 deg
meters
meters

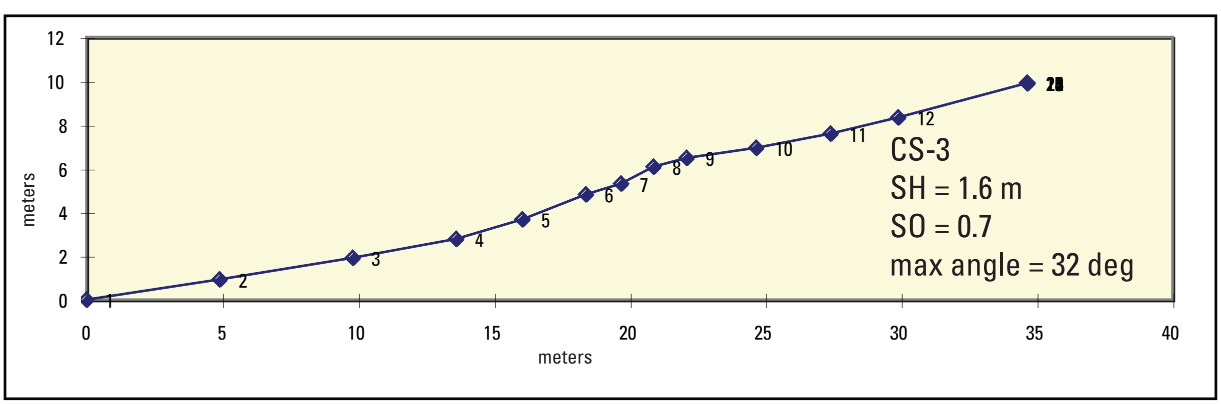
CS-3
SH = 1.6 m
SO = 0.7
max angle = 32 deg
meters
meters

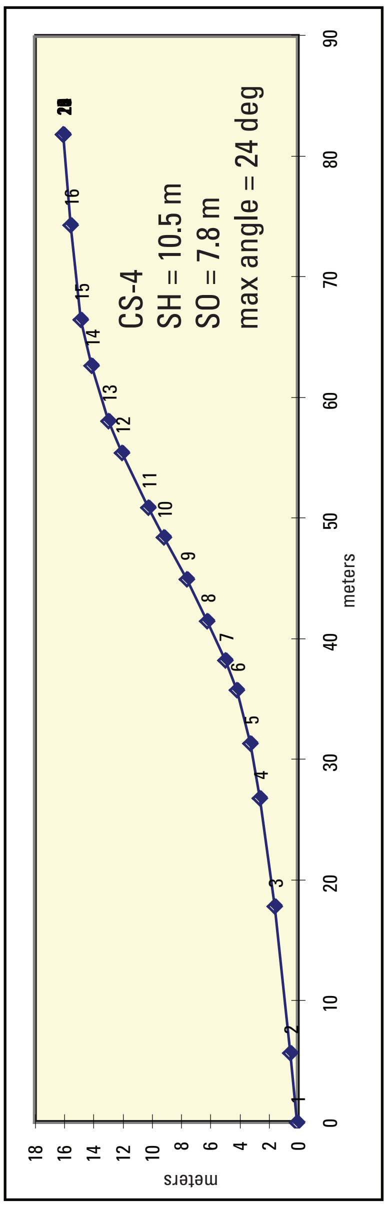
CS-4
SH = 10.5 m
SO = 7.8 m
max angle = 24 deg
meters
meters

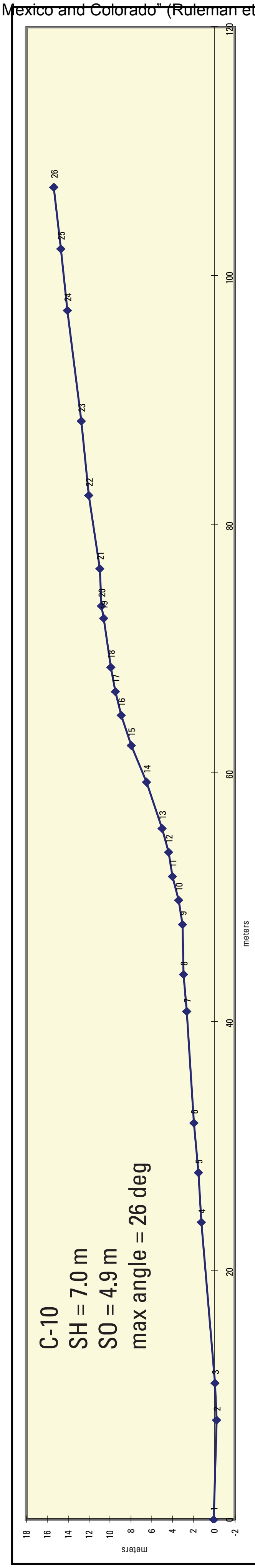
C-10
SH = 7.0 m
SO = 4.9 m
max angle = 26 deg
meters
meters

DR2013136 for GSA Special Paper 494, Chapter 3, "Late Miocene–Pleistocene evolution of a Rio Grande rift subbasin, Sunshine Valley–Costilla Plain, San Luis Basin, New Mexico and Colorado" (Ruleman et al.)

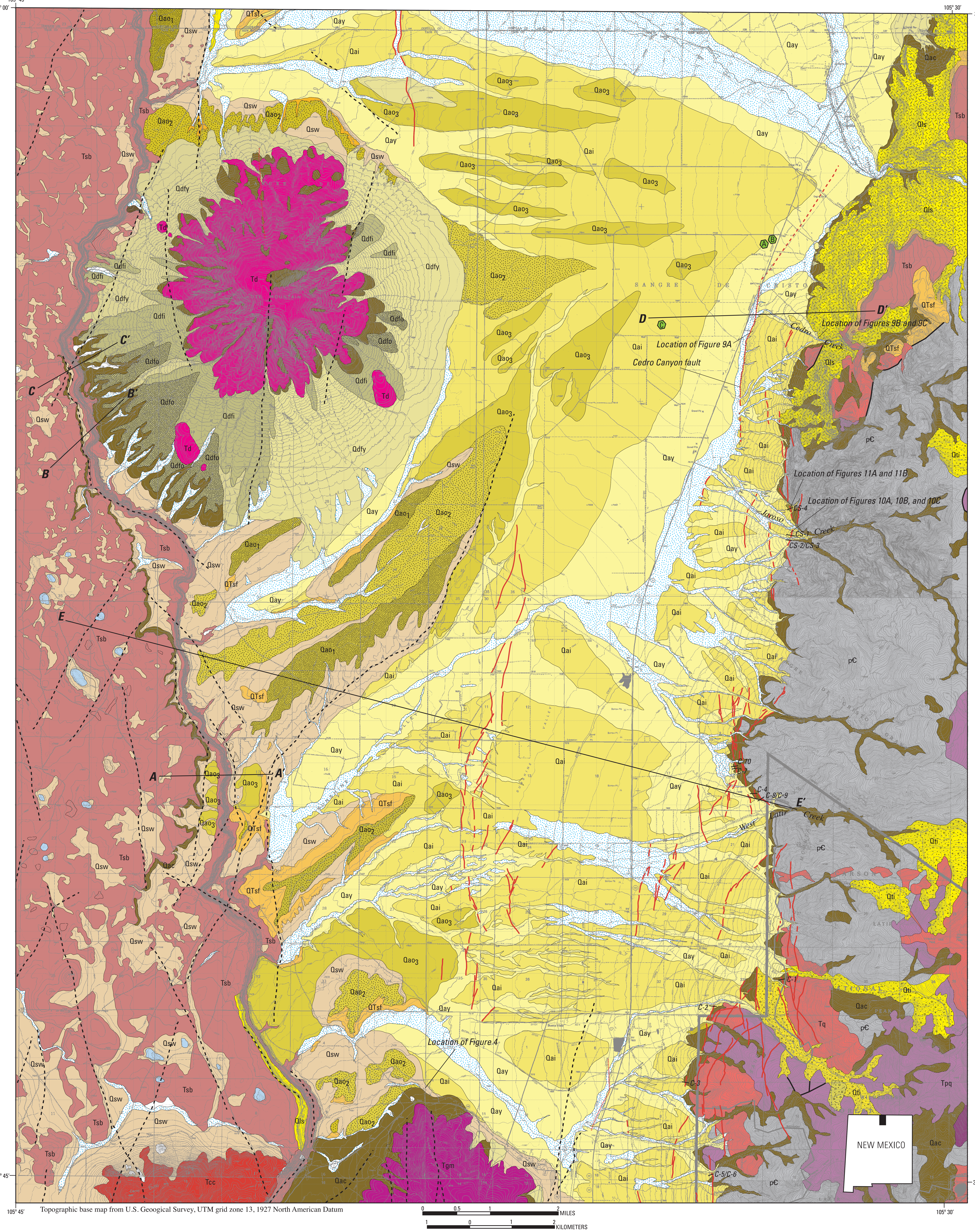

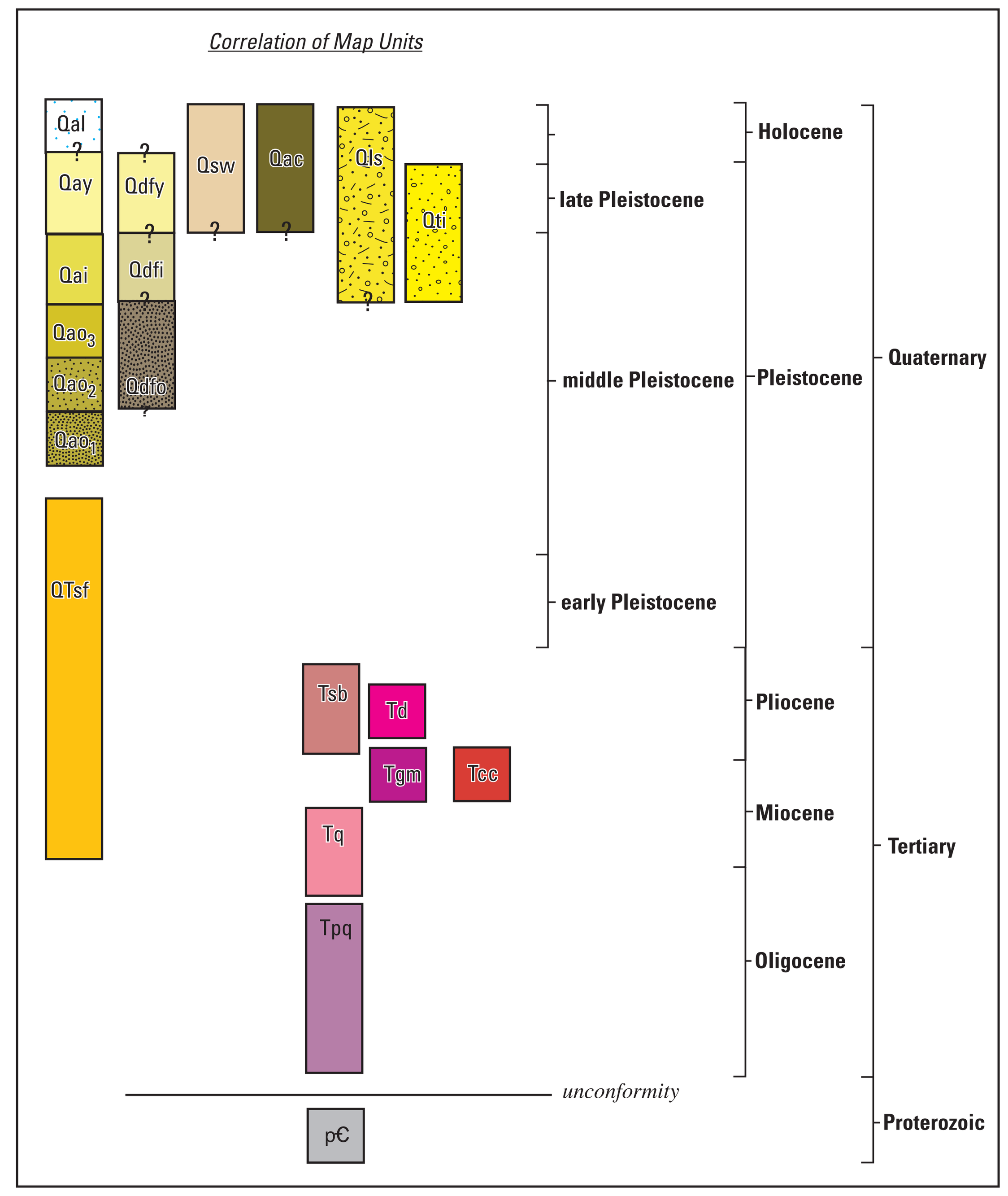

(See Manuscript for Unit Descriptions)

- Qal — Valley-floor alluvium (Holocene and late Pleistocene?)
- Qsw — Sheetwash alluvium (Holocene? and late Pleistocene)
- Qay — Younger piedmont alluvium (Holocene and late Pleistocene)
- Qai — Intermediate piedmont alluvium (middle Pleistocene)
- Qao_3 — Lower older piedmont alluvium (middle Pleistocene)
- Qao_2 — Higher Older Piedmont Alluvium (middle Pleistocene)
- Qao_1 — Highest older piedmont alluvium (middle Pleistocene)
- Qdfy — Younger debris flow deposits (late? Pleistocene)
- Qdfi — Intermediate debris flow deposits (late? middle Pleistocene)
- Qdfo — Older debris flow deposits (middle? Pleistocene)
- Qac — Alluvium and colluvium, undivided (Holocene and late? Pleistocene)
- Qls — Landslide deposits (Holocene to middle? Pleistocene)
- Qti — Glacial till (late and middle Pleistocene)
- QTsf — Santa Fe Group (middle Pleistocene to Miocene)
- Tsb — Servilleta Basalt and associated volcanic rocks (Pliocene 4.5-3.46 Ma)
- Td — Dacite and andesite of Ute Mountain (Pliocene 3.95 Ma)
- Tgm — Dacite of Guadalupe Mountain (Miocene 4.64 Ma)
- Tcc — Trachyandesite of Cerro Chiflo (Miocene 5.32±0.08)
- Tq — Volcanics of the Questa caldera complex within the Latir volcanic field (Miocene and Oligocene)
- Tpq — Pre-Questa Caldera volcanic rocks of the Latir volcanic field (Oligocene)
- p€ — Crystalline basement rocks undivided (Neoproterozoic? to Paleoproterozoic)
- B — Well location used for cross section D–D' on Figure 8
- C-3 — Fault scarp profile location
- Fault scarp
- Pliocene-early Pleistocene fault
- Pre-Pliocene fault

GEOLOGIC MAP OF SUNSHINE VALLEY-COSTILLA PLAIN REGION, TAOS COUNTY, NEW MEXICO

C.A. Ruleman, R.A. Thompson, and R.R. Shroba, U.S. Geological Survey

Plate 1.